Elastic electron-proton scattering: current status and perspectives

N.A. Kivel – *Institute für Theoretische Physik II, Ruhr-Universität Bochum, Research interests: chiral dynamics, hard exclusive processes, B-physics.*

Abstract: There has been much activity in the measurements of elastic electromagnetic proton and neutron form factors in the last decades. Here we provide short introduction to elastic electron-proton scattering and review present and future experiments dedicated to the measurements of the proton form factors. Some part of the lecture devoted to the two-photon mechanism which plays important role in explanation of the well known discrepancy in extraction of electric form factor G_E from the unpolarized and polarized experiments. This discrepancy has been known for the past several years and is currently the subject of intense theoretical discussion.

Elastic electron-proton scattering: current status and perspectives

Nikolay Kivel
Institute für Theoretische Physik II, Ruhr-Universität Bochum, D-44780 Bochum, Germany
Petersburg Nuclear Physics Institute, 188350 Gatchina, Russia
e-mail: nikolai.kivel@tp2.rub.de

Abstract

There has been much activity in the measurements of elastic electromagnetic proton and neutron form factors in the last decades. Here we provide short introduction to elastic electron-proton scattering and review present and future experiments dedicated to the measurements of the proton form factors. Some part of the lecture devoted to the two-photon mechanism which plays important role in explanation of the well known discrepancy in extraction of electric form factor G_E from the unpolarized and polarized experiments. This discrepancy has been known for the past several years and is currently the subject of intense theoretical discussion.

Introduction

Investigation of the structure of the nucleon is the one of the most important problem of the hadronic physics. The electromagnetic (e.m.) interaction provides a unique possibility to study experimentally in a cleanest way various aspects related with the nucleon structure. The measurements of different e.m. form factors in various inclusive (DIS, semi-inclusive DIS) and exclusive (elastic *ep*-scattering, DVSC) reactions provide us the fundamental information about the nucleon.

Historically, elastic electron-nucleon scattering was the first process used to study the spatial distribution of charge and magnetism carried by nucleon. The first experiments dedicated to form factor (FF) measurements of the proton were carried out at the Stanford University by Hofstadter and his team. The fist results were reported in 1955 for the proton FFs [1] and in 1958 [2] for the neutron magnetic FF. This experiments started new era in the investigation of hadrons. Information obtained about e.m. FFs from elastic experiments provides a lot of challenges both for experimentalists and theorists up to present time. The great progress have been made during last decade due to invention of the new experimental methods based on double polarized measurements (polarized beam and polarized target or polarized beam and

polarized recoiled proton). This technique allows to measure the ratio of e.m. FFs to a very high precision and provides important additional information to the classical unpolarized results. Such approach was used in the series experiments carried out at the Continuous Electron Beam Accelerator Facility of Jefferson Laboratory (JLab) in US in the last ten years. It was fond that measured ratio of electric to magnetic FFs behaves very differently, especially at large momentum transfer, compared to the similar results from unpolarized experiments. This discrepancy was clearly established and became the subject for many theoretical speculations about origin of the effect during last years. At present time, probably, the most realistic explanation is based on the computation of the so-called two photon exchange (TPE) diagrams which present the part of the e.m. radiative corrections. Unfortunately, this computation can not be done without any assumptions and therefore it involves certain theoretical models and ambiguities. On the other hand, there is a rich experimental program dedicated to the further investigations of nucleon FFs and also possible effects from the TPE at high momentum transfer. What is especially important, that expected data will have quite small experimental uncertainties.

In present lecture we provide short introduction to some aspects elastic electron-proton scattering at large momentum transfer and discuss certain theoretical developments related to the proton FFs. The main emphasis is made on the QCD factorization approach.

Extraction of the proton FFs from unpolarized and polarized experiments: current results

In present lecture we restrict our consideration by proton FFs. The amplitude of elastic scattering in the one photon approximation, see Fig.1 is given by

$$iM_\gamma = (-ie)\overline{u}_e(k')\gamma_\mu u_e(k)\,\frac{(-i)}{q^2}\,ieJ^\mu, \tag{1}$$

where J^μ denotes the proton transition current

$$J^\mu = \overline{N}(p')\left[\gamma^\mu F_1(Q^2) + \frac{i\sigma^{\mu\nu}\Delta_\nu}{2M}F_2(Q^2)\right]N(p). \tag{2}$$

We shall use M to denote the proton mass and $Q^2 = -q^2 = -(p'-p)^2$ is momentum transfer. Two independent FFs, F_1 and F_2 are real functions of Q^2 and in the static limit $Q^2 = 0$, $F_1(0) = 1$, $F_2(0) = \mu_p$, where $\mu_p = 2.79$ is the proton magnetic moment. In order to make physical interpretation for the FFs $F_{1,2}$ it is convenient to pass to Breit frame, defined by $\boldsymbol{p}' = -\boldsymbol{p}$.

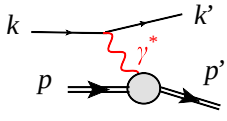

Figure 1: Elastic ep scattering

In this frame there is no energy transferred to the proton and it behaves as if it had bounced off a brick wall. Evaluating the four components of the proton current $eJ^\mu = (\rho, \boldsymbol{J})$ associated with charge and current distributions one obtains[1]

$$\rho = e2M\delta_{\lambda,-\lambda'}(F_1 - \frac{Q^2}{4M^2}F_2), \quad \boldsymbol{J}_1 \pm iJ_2 = \mp\delta_{\lambda,\lambda'}e2Q(F_1+F_2), \tag{3}$$

where λ, λ' denote the initial and final proton helicities, respectively. Corresponding combinations known as Sachs FFs ($\tau = \frac{Q^2}{4M^2}$)

$$G_E = (F_1 - \tau F_2), \quad G_M = F_1 + F_2, \tag{4}$$

can be associated with charge and magnetic current density distributions at small momentum transfer $Q \ll M$ through a Fourier transformation. One can easily find that the slope of the FF G_E can be interpreted as the mean square radius $\langle r^2\rangle$ of charge cloud:

$$G_E(Q^2) = \int d^3\boldsymbol{x} e^{i\boldsymbol{x}\boldsymbol{q}}\rho(\boldsymbol{x}) \simeq 1 + \frac{1}{6}Q^2\langle r^2\rangle + \dots. \tag{5}$$

with $Q^2 = -|\boldsymbol{q}|^2$. In particular, if the charge distribution $\rho(r)$ has an exponential form, $\rho(r) \sim e^{-\Lambda r}$, then one finds that $G_E(Q^2) = (1 - Q^2/\Lambda^2)^{-2}$ which is known as dipole distribution. Note however, that for large values of Q above interpretation is spoiled by relativistic corrections. Then one has to pass to the infinite momentum frame and define charge distribution in the transverse plane, see, for instance, [3].

The cross section for ep scattering, when written in terms of electric and magnetic FFs, G_E and G_M, takes the following form

$$\frac{d\sigma}{d\Omega_{\rm Lab}} = \left(\frac{d\sigma}{d\Omega_{\rm Lab}}\right)_{\rm ns} \frac{\tau}{\epsilon(1+\tau)}[G_M^2 + \frac{\epsilon}{\tau}G_E^2], \tag{6}$$

where $\tau \equiv Q^2/4M^2$ and ϵ is the virtual photon polarization parameter $\epsilon = [1 + 2(1+\tau)\tan^2\theta/2]^{-1}$, θ is the electron Lab scattering angle. The "no-structure" cross section is given by

$$\left(\frac{d\sigma}{d\Omega_{\rm Lab}}\right)_{\rm ns} = 4\alpha_{em}^2\cos^2(\theta/2)\frac{E'^3}{EQ^4}, \tag{7}$$

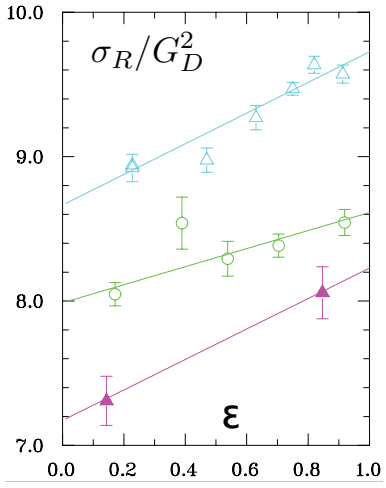

Figure 2: Rosenbluth separation based on the data from [9] for different Q^2 values, 2.5 (open triangles), 5.0 (circle), 7.0 (filled triangles) GeV^2.

[1] Assuming that z axis is chosen along $\boldsymbol{p}$ and helicity spinors are used.

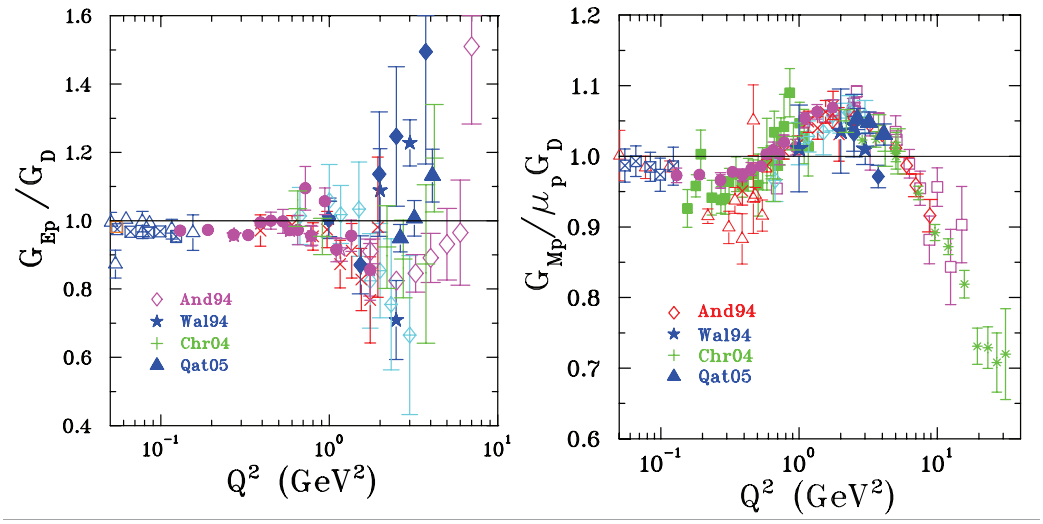

Figure 3: Data for G_E and G_M obtained by the Rosenbluth separation method. The full set of references on the data can be fond in [4].

where E and E' are incoming and outgoing electron Lab energies. The Rosenbluth separation technique takes advantage of the linear dependence in ϵ of the FFs in reduced cross section defined as

$$\sigma_R = G_M^2 + \frac{\epsilon}{\tau} G_E^2 = \frac{\epsilon(1+\tau)}{\tau} \left(\frac{d\sigma}{d\Omega}\right)_{\rm exp} / \left(\frac{d\sigma}{d\Omega}\right)_{\rm ns} . \tag{8}$$

Performing the linear fit of several measured reduced cross section values at fixed Q^2 one obtains G_E^2/τ as the slope and G_M^2 as the intercept. In Fig.2 we demonstrate such fit for several values Q^2, the data are taken from [9]. The reduced cross section is divided by dipole FF G_D defined as $G_D = (1+Q^2/0.71{\rm GeV}^2)^{-2}$. In Fig.3 we show the compilation of the G_E and G_M obtained by Rosenbluth separation technique. Again, both FFs are divided by dipole FF G_D. As one can see from Fig.3, the description G_E becomes very problematic above $Q^2 \sim 1{\rm GeV}^2$. This can be explained by the fact that extraction of G_E is very difficult at large Q^2 due to several reasons. First, suppression by factor $1/\tau$ in front of G_E^2 in Eq. (8); and second, even at small Q^2 taking into account that $G_M^2 \sim \mu_p^2 G_E^2$ we find that the term with G_E^2 is numerically reduced by factor $\mu_p^2 \simeq 7.8$. In case of magnetic FF G_M the situation is better and one can observe the clearly decreasing of the ratio $G_M/\mu_p G_D$ at Q^2 above $5{\rm GeV}^2$.

The measurements of G_E at large Q^2 can be essentially improved in the recoil polarization experiments when a longitudinally polarized beam of electrons is scattered by unpolarized protons. For one photon exchange, in the $\boldsymbol{e} + p \to e + \boldsymbol{p}$ reaction, see Fig.4, the scattering of polarized electrons results in a transfer of polarization to the

recoil proton with only two non-zero components, P_t perpendicular to, and P_l parallel to the proton momentum in the scattering plane. The polarized cross section is given by

$$\frac{d\sigma_{pol}}{d\sigma_{unpol}} = 1 + h\boldsymbol{S}_p \cdot \boldsymbol{P},\ \ \boldsymbol{P} = (P_x, P_y = 0, P_z) = \\ = \left(-\sqrt{\frac{2\epsilon(1-\epsilon)}{\tau}}\,\frac{G_E G_M}{\sigma_R},\ 0,\ \sqrt{1-\epsilon^2}\,\frac{G_M^2}{\sigma_R} \right), \tag{9}$$

where $\boldsymbol{S}_p$ denote the recoil proton polarization. From these formulas it follows that the FF ratio can be extracted from the ratio of the measured polarizations:

$$\frac{P_x}{P_z} \equiv \frac{P_t}{P_l} = -\sqrt{\frac{2\epsilon}{\tau(1+\epsilon)}}\,\frac{G_E}{G_M}. \tag{10}$$

Practically, such a method has several advantages over the Rosenbluth technique. First, only single measurement is required for given Q^2 (if the both components can be measured at the same time). This allows to reduce the systematic errors associated with angle and beam energy change. Second, ambiguities related with the normalization of the absolute cross section also cancel in the ratio.

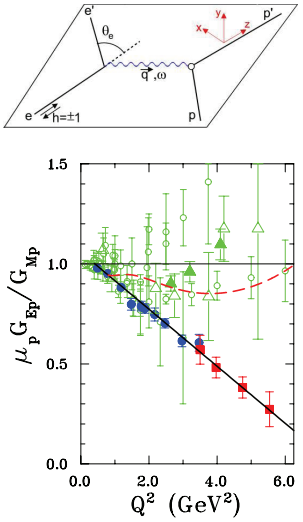

Figure 4: Upper figure: kinematics of polarized process. Bottom plot: Comparison of the e.m. FFs ratio from the JLab polarization data and Rosenbluth separation. Dashed curve is a re-fit of Rosenbluth data from [12].

Such experiments has been carried out at different values of Q^2 in JLab [6, 7, 8]. Their results, for the first time showed a clear deviation of the proton FF ratio from unity, starting from $Q^2 > 1\text{GeV}^2$ with much smaller statistical and systematical errors compare to previous similar measurements, see more detailed discussion in [4]. In Fig.4 the obtained results for the ratio G_E/G_M from polarization experiments are shown together with results obtained from the Rosenbluth separation method. Moreover, two JLab collaborations (Hall-A and Hall-C) repeated unpolarized experiments and extracted the ratio using the Rosenbluth technique [10, 11]; their results are shown in Fig.4 as open and filled triangles, respectively. As one can see these results are in agreement with the previous unpolarized data. From the given picture we observe the clear discrepancy between the ratios obtained with the Rosenbluth separation and the recoil polarization method. Careful re-analysis made in [12] allows to conclude that the difference can not be explained by either simple re-normalization of the Rosenbluth data or by variation of the polarization data within the quoted experi-

mental uncertainties. Let us also add, that recently a new experiment [13] has measured the G_E/G_M ratio at $Q^2 = 2.5 - 8.5\text{GeV}^2$. Preliminary data has been presented in workshop [14]. New results are in agreement with previous measurements in the overlap region but show clear deviation from the simple linear fit at $Q^2 > 6\text{GeV}^2$.

This discrepancy has been known for the past several years and is currently the subject of intense discussion. At present time, the most realistic explanation of this discrepancy is based on the effect produced by the two photon exchange (TPE) radiative corrections which we are going to discuss below. Practically, is it very difficult to compute TPE from the first principles. There are several approaches suggested to estimate TPE effect and based on different ideas about hadron dynamics.

At the same time TPE mechanism can be studied experimentally and at present time there is already rich program consisting of set of different experiments which can help us clearly to conclude about the importance of TPE and constrain the underlying dynamics. Let us mention some of them.

The real part of the TPE amplitude can be accessed directly as the deviation from unity of the ratio of e^+/e^- elastic scattering. It is easy to see that this ratio can be written as

$$\frac{d\sigma_{e^+p}}{d\sigma_{e^-p}} \simeq 1 + 4\text{Re}M_{\gamma\gamma}/M_\gamma, \tag{11}$$

where M_γ and $M_{\gamma\gamma}$ denote the amplitudes with one and two gamma exchange respectively. The precision of past experiments performed at SLAC [15], was not sufficient to see a clear deviation from unity over a large range in ε. Presently, several new experiments are planned or are underway at VEPP-3 [16], JLab/CLAS [17], and Olympus@DESY [18] to make precision measurements of the e^+/e^- ratio in elastic scattering off a proton. The Olympus@DESY experiment aims at a statistical precision of the e^+/e^- cross section ratio of better than one percent for an average $Q^2 = 2.2$ GeV^2.

The imaginary part of TPE can be accessed through single spin asymmetries. In the recent experiment [19] target normal spin asymmetry has been measured at $Q^2 = 1.0,\ 2.3\text{GeV}^2$, the data is currently under analysis.

At the end of experimental review let us mention about future important experiments dedicated to the FF measurement. Among approved JLab experiments which are planned to carry out after 12 GeV CEBAF upgrade we mention measurements of G_E/G_M in Hall A at $Q^2 = 6 - 14.8\text{GeV}^2$ [21] and in Hall C at $Q^2 = 6 - 13\text{GeV}^2$ [20]. There will be also very precise measurements of the unpolarized reduced cross section in Hall A [22] at $Q^2 = 7 - 17.5\text{GeV}^2$ with the total accuracy smaller then 2%. Here we mention only experiments with the proton target. The complete list of the planned measurements can be find on the site of JLab [23].

As one can see from above, the future measurements will reach quite large values of Q^2 and it will provide us very interesting information about the structure of proton

at small distances. In particular, it will allow us to test the QCD predictions for asymptotic of e.m. FFs developed on the basis of the so-called QCD factorization approach. In next section we briefly review this topic in connection with the TPE mechanism.

Two photon exchange mechanism in QCD factorization approach

We start this section from the discussion of the e.m. radiative corrections (RC). In all experiments the measured raw cross sections have to be corrected to first order in $\alpha_{em} \sim 1/137$, before accessing one photon exchange (or Born) cross section $d\sigma_{\rm raw} = d\sigma_{Born}(1+\delta_{RC})$. Important that such corrections depend on Q^2 and ϵ. In the current energy range of JLab effect from RC is typically of order $15-30\%$. Such relatively large contribution is explained by enhancement due to large logarithms $\delta \sim \ln[Q^2/m_e^2]\ln[4EE'/\Delta E]$ from the pure QED loops and soft photon emissions. The details can be fond in [24, 25]. The fact that this effect is ϵ-dependent is very important for the extraction of G_E (given by the slope versus ϵ) from the unpolarized data. In Fig.5 one can see the effect of RC for the reduced cross section for the several values of Q^2. From this picture one can clearly observe that the final value of G_E^2 obtained from the reduced cross section data is defined by the value and accuracy of the ϵ-dependent part of the radiative correction. This is especially important because the discrepancy between the Rosenbluth linear fit and the recoil polarization data is in the range of $4-7\%$.

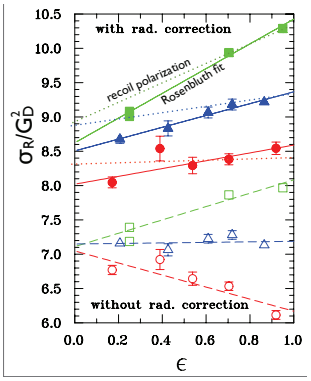

Figure 5: Rosenbluth plot for data [9]. At bottom before RC, at top after RC. Filled squares, triangles and circles for 1.75, 3.25, 5GeV^2, respectively. empty symbols for uncorrected data; dotted lines denote recoil polarization slope.

Therefore, it is natural to assume that the solution of the discrepancy between two measurements can be done by careful re-examination of the RC. It was fond that the one of the most suspicious moment which can potentially provide sensitive effect for slope is the calculation of the TPE or box diagrams. In the previous calculations [24] these diagrams were computed in the so-called "soft photon approximation". In this case the effect of the proton structure was neglected; in considering the proton legs, only the soft virtual photon contribution is calculated exactly - approximations are made in the hard virtual photon contribution. In [25] the effect of the proton internal structure was estimated by inserting the vertices with the nontrivial proton FFs. Again, some approximations were done for the box diagrams. It was fond that the resulting effect is small.

However, more realistic calculation beyond Born approximation are required in order to demonstrate quantitatively that TPE effect are indeed able to resolve the discrepancy. Last few years several model calculations of TPE amplitude have been suggested. Discussion of these calculations is going beyond of our presentation and the interested reader can find more detailed information and references in review papers [4, 5]. Recently, a more sophisticated method was used to estimate TPE amplitude at large Q^2 limit. This approach is based on QCD technique developed for hard exclusive reactions. Below we discuss this idea in detail.

At large values of the total energy s and momentum transfer Q^2 elastic scattering can be considered as a hard process and its asymptotic can be computed on the basis of the so-called factorization approach based on the asymptotic freedom of QCD. The basic idea of the approach is to separate the short and long distance dynamics. Then the short distance part describes the parton scattering with large momenta $\mu_F^2 \le k_i^2 \le Q^2$ and can be computed using perturbative QCD. The scale μ_F is the so-called factorization scale, which separates soft and hard regimes. Then the soft part describes the scattering with the soft momenta $\Lambda_{QCD}^2 \le k_i^2 \le \mu_F^2$. Usually, such non-perturbative subprocess is described by certain matrix elements of a light-cone operator between hadronic states.

Factorization approach has been developed for the nucleon FFs long time ago, see reviews in [26, 27] and references therein. Let us shortly discuss obtained results. In the hard regime, where $Q^2, s \gg M^2$, it is convenient to calculate the amplitude in the Breit system, where the initial and final proton momenta have large components $\sim Q$ and correspond to two opposite light-like directions:

$$p \simeq (Q/2)\,\overline{n},\; p' \simeq (Q/2)\,n,\;\text{ with } \overline{n} = (1,0,0,1),\; n = (1,0,0,-1),\;\text{ and } (n\cdot\overline{n}) = 2. \tag{12}$$

According to factorization theorem, Dirac FF F_1 (2) can be represented as convolution integral of the soft and hard parts with respect to momentum fractions $x_i \equiv \{x_1, x_2, x_3\}$ and $y_i \equiv \{y_1, y_2, y_3\}$ of initial and final protons, respectively:

$$F_1(Q^2) = \frac{(4\pi\alpha_s(\mu_R^2))^2}{54Q^4}\int d[x_i]\int d[y_i]\,\{\varphi_N(x_i)A[x_i,y_i]\varphi_N(y_i) + T(x_i)B[x_i,y_i]T(y_i)\}\,, \tag{13}$$

where $d[x_i] \equiv dx_1dx_2dx_3\delta(1-\sum x_i)$. The hard scattering amplitudes A, B are given by rational functions of the momentum fractions ($\overline{x}_i \equiv 1 - x_i$)

$$A[x_i,y_i] = \frac{2e_u}{\overline{x}_1^2x_3\overline{y}_1^2y_3} + \frac{2e_d}{x_2\overline{x}_3^2y_2y_3^2} + \dots, \tag{14}$$

$$B[x_i,y_i] = \frac{8e_u}{\overline{x}_1^2x_3\overline{y}_1^2y_3} + \frac{4e_d}{x_1\overline{x}_1x_2y_1y_2\overline{y}_2} + \dots, \tag{15}$$

where the dots denote the others similar contributions. The full result can be fond, for instance, in [26]. Corresponding expressions were computed from the Feynman diagrams describing the hard process of the quark-photon scattering $u(x_1p)u(x_2p)d(x_3p)+$

$\gamma^* \to u(y_1p')u(y_2p')d(y_3p')$ at tree level. The typical diagram is shown in Fig. 6. Two

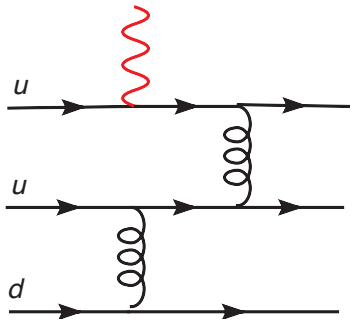

Figure 6: Typical diagram for the hard scattering amplitude in case of proton FF.

gluon exchange Born diagrams represent the simplest configurations which possible in this case. This can be easily understood at large Q^2 in the Breit frame introduced above. Then one can observe that initial and final quarks are collinear particles moving along z-axis but in opposite directions. In order to invert the direction of motion of the initial quark on must introduce elementary scattering with hard gluon or photon. For three initial quarks we need one photon and 2 gluons and corresponding diagrams provide the leading order result.

The functions φ_N and T in Eq. (13) are nucleon Distribution Amplitudes (DAs). These are non-perturbative quantities describing how the large longitudinal momentum of the proton is sheared between their constituents. These functions are defined as a twist-3 matrix element of the light-cone 3-quark operators. Following the notation from [28], the corresponding proton matrix element is given:

$$4\left\langle 0\left|\varepsilon^{ijk}u^i_\alpha(a_1\lambda n)u^j_\beta(a_2\lambda n)d^k_\sigma(a_3\lambda n)\right|p\right\rangle = V\ p^+\left[\left(\tfrac{1}{2}\overline{n}\cdot\gamma\right)\ C\right]_{\alpha\beta}\left[\gamma_5 N^+\right]_\sigma$$
$$+A\ p^+\left[\left(\tfrac{1}{2}\overline{n}\cdot\gamma\right)\gamma_5 C\right]_{\alpha\beta}\left[N^+\right]_\sigma + T\ p^+\left[\tfrac{1}{2}i\sigma_{\perp\overline{n}}\ C\right]_{\alpha\beta}\left[\gamma^\perp\gamma_5 N^+\right]_\sigma, \qquad (16)$$

with light-cone momentum $p^+ \equiv (p\cdot n) = Q$, where C is charge conjugation matrix: $C^{-1}\gamma_\mu C = -\gamma_\mu^T$, and where $X = \{A, V, T\}$ stand for the nucleon DAs which are defined by the light-cone matrix element

$$X(a_i, \lambda p^+) = \int d[x_i]\ e^{-i\lambda p^+(\sum x_i a_i)}X(x_i).$$

In general, the following properties are valid:

$$\begin{aligned} V(x_i) &= \tfrac{1}{2}(\varphi_N(x_1,x_2,x_3) + \varphi_N(x_2,x_1,x_3)),\\ A(x_i) &= \tfrac{1}{2}(\varphi_N(x_1,x_2,x_3) - \varphi_N(x_2,x_1,x_3)),\\ T(x_i) &= \tfrac{1}{2}\left[V-A\right](1,3,2) + \tfrac{1}{2}\left[V-A\right](2,3,1), \end{aligned}$$

i.e. we have only one independent function φ_N.

The second, helicity flip Pauli FF F_2 is stronger suppressed at large Q^2

$$F_2(Q^2) \sim 1/Q^6. \tag{17}$$

Its factorized expression involves the DAs of twist-4 and corresponding convolution integrals are divergent in the end-point region $x_i \sim 0$ or $x_i \sim 1$. This means that F_2 can not be represented in such simple factorized form like F_1.

Phenomenological analysis of the available data for e.m. FFs at moderate values of $Q^2 < 10\text{GeV}^2$ shows that the leading order asymptotic regime is still not working in this region, see, for instance, discussions in [29]. In order to describe the data for such values of Q^2 one has to involve asymptotically suppressed power corrections. The important role in this case plays the so-called soft overlap configurations: when the hard scattering involves only one active quark, and FF is obtained as an overlap of initial and final hadron wave functions. The hard scattering mechanism, on the other hand, involves two gluon exchange and proportional to $\sim \alpha_s^2(\mu_R^2)$. The scale of the running coupling $\mu_R^2 = cQ^2$, where c is some number which can be obtained from the next-to-leading calculation. Most probably, this number is quite small, because of hard momentum Q^2 is diluted between the few propagators and therefore the asymptotic regime can be accessed only at sufficiently high $Q^2 > 10\text{GeV}^2$. Therefore despite the soft mechanism is suppressed asymptotically by a power of $1/Q^2$ relative to the hard scattering mechanism, it may well dominate at accessible values of Q^2. Such picture is quite well supported by recent calculations in framework of light-cone QCD sum rules [30].

It is very interesting to perform the similar analysis for the TPE mechanism, especially in view of future experiments with quite large values of Q^2. For this case we choose again Breit system as described in (12). Then the lepton kinematics are given by $k = \zeta(Q/2)\, n - \overline{\zeta}(Q/2)\, \overline{n} + k_\perp$, and $k' = -\overline{\zeta}(Q/2)\, n + \zeta(Q/2)\, \overline{n} + k_\perp$, where, at large Q^2, $s \simeq \zeta Q^2$, and $u \simeq \overline{\zeta} Q^2$, with $\overline{\zeta} \equiv 1 - \zeta$, and $\zeta \geq 1$. Furthermore, the transverse vector in the lepton kinematics is determined from $k_\perp^2 = -\zeta\overline{\zeta} Q^2$. To describe the elastic ep scattering, $l(k) + N(p) \to l(k') + N(p')$, we adopt the definitions $P = (p + p')/2$, $K = (k + k')/2$, $q = k - k' = p' - p$, and choose $s/Q^2 = \zeta > 1$ and $\nu = K \cdot P$ as the independent kinematic invariants. Neglecting the electron mass, it was shown in [31] that the T-matrix for elastic ep scattering can be expressed through 3 independent Lorentz structures as

$$T = \frac{e^2}{Q^2}\, \overline{u}(k')\gamma_\mu u(k)\, \overline{u}(p') \left(\tilde{G}_M\, \gamma^\mu - \tilde{F}_2 \frac{P^\mu}{M} + \tilde{F}_3 \frac{\gamma \cdot K P^\mu}{M^2} \right) u(p), \tag{18}$$

In Eq. (18), $\tilde{G}_M$, $\tilde{F}_2$, $\tilde{F}_3$ are complex functions of ν and Q^2. To separate the 1γ and 2γ exchange contributions, it is furthermore useful to introduce the decompositions: $\tilde{G}_M = G_M + \delta\tilde{G}_M$, and $\tilde{F}_2 = F_2 + \delta\tilde{F}_2$. The amplitudes $\tilde{F}_3, \delta\tilde{G}_M$ and $\delta\tilde{F}_2$

originate from processes involving at least 2γ exchange and are of order e^2 (relative to the factor e^2 in Eq. (18)).

In the hard regime, where $Q^2, s = (k+p)^2 \gg M^2$ and $s/Q^2 = \zeta$ is fixed, contribution to the 2γ exchange correction to the elastic ep amplitude is given by a convolution integral of the proton distribution amplitudes (DAs) with the hard coefficient function as shown in Fig. 7. Such hard scattering picture is very similar to the

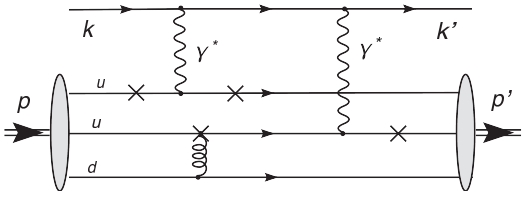

Figure 7: Typical graph for the elastic ep scattering with two hard photon exchanges. The crosses indicate the other possibilities to attach the gluon. The third quark is conventionally chosen as the $d-$quark. There are other diagrams where the one photon is connected with $u-$ and $d-$ quarks. We do not show these graphs for simplicity.

situation with FFs discussed above except that now we have 2 hard photons and only one hard gluon exchange. Therefore, in contrast to the FFs, the result is proportional to $\alpha_s(\mu_R^2)$. That allows us to assume, that the corresponding contribution might be quite important already at moderate values of Q^2.

In the large Q^2 limit, the pQCD calculation of Fig. 7 involves 24 diagrams, and leads to hard 2γ corrections to $\delta\tilde{G}_M$, and $\nu/M^2\tilde{F}_3$, which are found as [32]:

$$\delta\tilde{G}_M = -\frac{\alpha_{em}\alpha_S(\mu_R^2)}{Q^4}\left(\frac{4\pi}{3!}\right)^2 (2\zeta-1)\int d[y_i]\; d[x_i]\,\frac{4\,x_2\,y_2}{D}\{\dots\}, \tag{19}$$

$$\frac{\nu}{M^2}\tilde{F}_3 = -\frac{\alpha_{em}\alpha_S(\mu_R^2)}{Q^4}\left(\frac{4\pi}{3!}\right)^2 (2\zeta-1)\int d[y_i]\; d[x_i]\,\frac{2(x_2\,\overline{y}_2+\overline{x}_2\,y_2)}{D}\{\dots\}, \tag{20}$$

where

$$\{\dots\} = 2Q_uQ_d\,[V'V+A'A]\,(1,3,2) + {Q_u}^2\,[(V'+A')(V+A)+4T'T]\,(3,2,1) \\ +Q_uQ_d\,[(V'+A')(V+A)+4T'T]\,(1,2,3), \tag{21}$$

with quark charges $Q_u = +2/3$, $Q_d = -1/3$ and the denominator factor D is defined as

$$D \;\equiv\; (y_1y_2\overline{y}_2)\,(x_1x_2\overline{x}_2)\,\left[x_2\overline{\zeta}+y_2\zeta-x_2y_2+i\varepsilon\right]\left[x_2\zeta+y_2\overline{\zeta}-x_2y_2+i\varepsilon\right]. \tag{22}$$

The unprimed (primed) quantities in Eqs. (19, 20) refer to the DAs in the initial (final) proton respectively. One notices that at large Q^2, the leading behavior for $\delta\tilde{G}_M$ and $\nu/M^2\tilde{F}_3$ goes as $1/Q^4$. In contrast, the invariant $\delta\tilde{F}_2$ is suppressed in this

limit and behaves as $1/Q^6$. The similar calculation (up to normalization factor) was also reported in [33].

To evaluate the convolution integrals in Eqs. (19, 20), we need to insert a model for the nucleon twist-3 DAs φ_N. The asymptotic behavior of the DA and their first conformal moments were given in [28] as

$$\varphi_N(x_i) \simeq 120 x_1 x_2 x_3 f_N \left[1 + r_-(x_2 - x_1) + r_+(1 - 3x_3)\right], \tag{23}$$

and depend on three parameters: f_N, r_- and r_+. In this work, we will provide calculations using two models for the DAs that were discussed in the literature. The corresponding parameters (at $\mu = 1$ GeV) read COZ [34]: $f_N = 5.0 \pm 0.5$, $r_- = 4.0 \pm 1.5$, $r_+ = 1.1 \pm 0.3$ and BLW [30]: $f_N = 5.0 \pm 0.5$, $r_- = 1.37$, $r_+ = 0.35$.

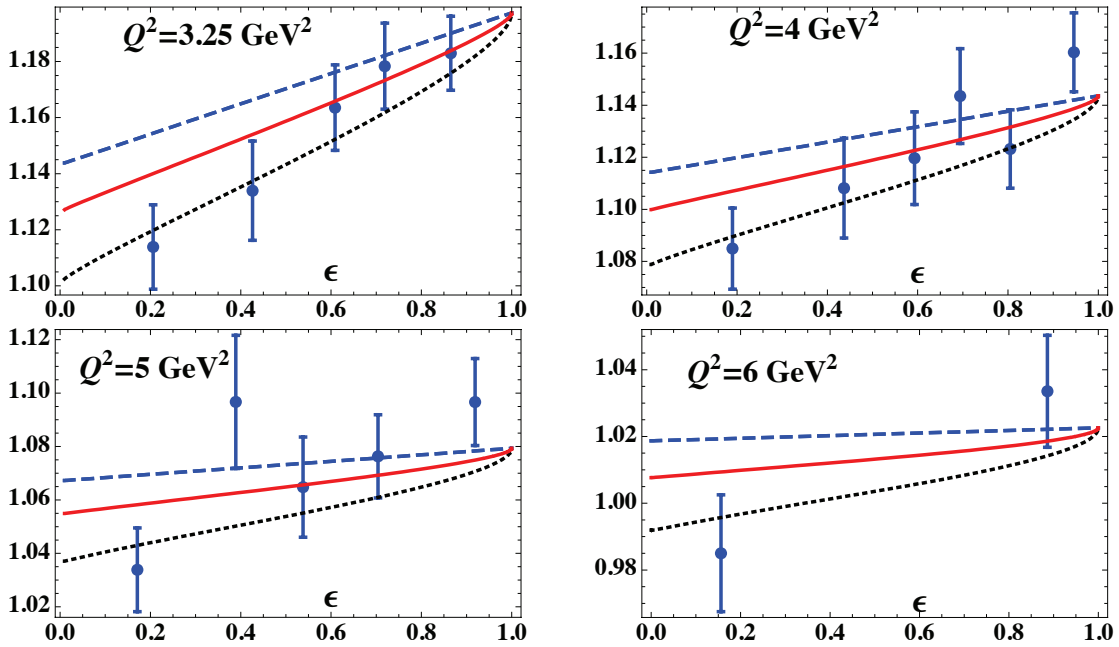

Figure 8: Rosenbluth plots for elastic ep scattering: σ_R divided by $\mu_p^2/(1+Q^2/0.71)^4$. Dashed (blue) curves: 1γ exchange, using the G_{Ep}/G_{Mp} ratio from polarization data [6, 7, 8] and empirical parametrization for G_{Mp} from [35]. Solid red (dotted black) curves show the effect including hard 2γ exchange calculated with the BLW (COZ) model for the proton DAs. The data are from Ref. [9].

We next calculate the effect of hard 2γ exchange, given through Eqs. (19, 20), on the elastic ep scattering observables. The general formulas for the observables including the 2γ corrections $\delta\tilde{G}_M$, $\delta\tilde{F}_2$, and $\nu/M^2\tilde{F}_3$ were derived in [31], to which we refer for the corresponding expressions. We assume that perturbative expansion at moderate Q^2 region is already applicable and fix the renormalization scale to be $\mu^2 = 0.6Q^2$ for each value of Q^2 shown below. In Fig. 8, we calculate the reduced cross

section σ_R as a function of the photon polarization parameter ε and different values of Q^2. In the 1γ exchange, $\sigma_R = G_M(Q^2) + \varepsilon/\tau\ G_E(Q^2)$, with $\tau = Q^2/(4M^2)$, and the Rosenbluth plot is linear in ε, indicated by the dashed straight lines in Fig.8. The effect including the hard 2γ exchange is shown for both the COZ and BLW models of the proton DAs. One sees that including the 2γ exchange changes the slope of the Rosenbluth plot, and that sizable non-linearities only occur for ε close to 1. The inclusion of the hard 2γ exchange is able to well describe the Q^2 dependence of the unpolarized data, when using the polarization data [6, 7, 8] for the proton FF ratio G_{Ep}/G_{Mp} as input. Quantitatively, the COZ model for the nucleon DA leads to a correction about twice as large as when using the BLW model. We like to note here that in contrast to the pQCD treatment of the proton FFs, which requires two hard gluon exchanges, the 2γ correction to elastic ep scattering only requires one hard gluon exchange. One therefore expects the pQCD calculation to set in for Q^2 values in the few GeV^2 range, which, probably, is confirmed by the results shown in Fig. 8. More detailed discussion of various observables can be fond in [32].

Bibliography

[1] R. Hofstadter and R.W. McAllister, Phys. Rev. **98**, 217 (1955).
R. Hofstadter, Rev. Mod. Phys. **28**, 214 (1956).

[2] M.R. Yearian, R. Hofstadter, Phys. Rev. **110**, 552 (1958).

[3] G.A. Miller, Phys. Rev. Lett. **99**, 112001 (2007) [arXiv:0705.2409 [nucl-th]].

[4] C.F. Perdrisat, V. Punjabi and M. Vanderhaeghen, Prog. Part. Nucl. Phys. **59**, 694 (2007) [arXiv:hep-ph/0612014].

[5] C.E. Carlson and M. Vanderhaeghen, Ann. Rev. Nucl. Part. Sci. **57**, 171 (2007).

[6] M.K. Jones *et al.* [Jefferson Lab Hall A Collaboration], Phys. Rev. Lett. **84**, 1398 (2000).

[7] V. Punjabi et al., Phys. Rev. C **71**, 055202 (2005) [Erratum-ibid. C 71:069902 (2005)].

[8] O. Gayou *et al.* [Jefferson Lab Hall A Collaboration], Phys. Rev. Lett. **88**, 092301 (2002).

[9] L. Andivahis *et al.*, Phys. Rev. D **50**, 5491 (1994).

[10] I.A. Qattan *et al.*, Phys. Rev. Lett. **94**, 142301 (2005) [arXiv:nucl-ex/0410010].

[11] M.E. Christy *et al.* [E94110 Collaboration], Phys. Rev. C **70** (2004) 015206 [arXiv:nucl-ex/0401030].

[12] J. Arrington, Phys. Rev. C **68** (2003) 034325 [arXiv:nucl-ex/0305009].

[13] JLab/Hall C exp. E-04-019, spokespersons R. Gilman, L. Pentchev, C. Perdrisat, and R. Suleiman.

[14] Talk given at XIII workshop on higher energy spin physics, Dubna, September 1-5, 2009, http://theor.jinr.ru/%7Espin/2009/spin09talks/3.09_Morning/Punjabi.pdf

[15] J. Mar *et al.*, Phys. Rev. Lett. **21**, 482 (1968).

[16] J. Arrington *et al.*, Proposal at VEPP-3, arXiv:nucl-ex/0408020.

[17] JLab/CLAS exp. E-04-116, spokespersons A. Afanasev, J. Arrington, W. Brooks, K. Joo, B. Raue, L. Weinstein.

[18] Proposal at DESY [Olympus Collaboration], (2008).

[19] JLab/Hall A exp. E-05-15, spokespersons T. Averett, X. Jiang, J.P. Chen.

[20] JLab/Hall A exp. E-1207-109, spokespersons E. Cisbani, E. Khandaker, L. Pentchev, C. Perdrisat, V. Punjabi, B. Wojtsekhowski.

[21] JLab/Hall C exp. E-1209-001, spokespersons E. Brash, M. Jones, V. Punjabi, C. Perdrisat.

[22] JLab/Hall A exp. E-1207-108, spokespersons J. Arrington, S. Gilad, B. Moffit, B. Wojtsekhowski.

[23] See for instance, http://www.jlab.org/div_dept/physics_division/experiments/ and http://www.jlab.org/exp_prog/12GEV_EXP/

[24] L.W. Mo and Y.S. Tsai, Rev. Mod. Phys. **41** (1969) 205.

[25] L.C. Maximon and J.A. Tjon, Phys. Rev. C **62**, 054320 (2000) [arXiv:nucl-th/0002058].

[26] V.L. Chernyak and A.R. Zhitnitsky, Phys. Rept. **112**, 173 (1984).

[27] G.P. Lepage and S.J. Brodsky, Phys. Rev. D **22**, 2157 (1980).

[28] V. Braun, R.J. Fries, N. Mahnke and E. Stein, Nucl. Phys. B **589**, 381 (2000) [Erratum-ibid. B **607**, 433 (2001)].